Convergence Analysis of Narrowband Active Noise Control

Sen M. Kuo[1], Ajay B. Puvvala[1] and Woon S. Gan[2]
[1]Department of Electrical Engineering, Northern Illinois University
Dekalb, IL 60115, kuo@ceet.niu.edu
[2]School of Electrical & Electronic Engineering,
Nanyang Technological University, Singapore 639798.

ABSTRACT

A narrowband feedforward active noise control (ANC) system consists of an adaptive filter excited by the sum of multiple sinusoids corresponding to the harmonic frequencies of the primary noise. The convergence of this direct-form ANC system is dependent on the frequency separation between two adjacent sinusoids in the reference signal. The analysis also proves that the length of the adaptive filter required for achieving the same convergence speed decreases with an increase in frequency separation. Computer simulations are conducted to verify the analysis presented in the paper.

1. INTRODUCTION

In many practical ANC applications [1, 2], the primary noise produced by rotating machines, such as engines, is periodic and contains multiple harmonic-related narrowband components. In these applications, the reference microphone can be replaced by a nonacoustic sensor such as a tachometer or an accelerometer [3] to synchronize an internally generated reference signal, thus preventing the feedback from the secondary source to the reference sensor. This periodic ANC system was analyzed in [4] using the filtered-X LMS (FXLMS) algorithm [5].

An adaptive sinusoidal interference canceller using a sinusoidal reference signal and two adaptive weights is developed in [6]. In practical applications, periodic noise usually contains multiple tones at the fundamental and several dominant harmonic frequencies. Glover [7] applies a sum of sinusoids as a reference signal to an adaptive filter with length much higher than two. The effect of the secondary path on the transfer function of the adaptive filter and its stability was analyzed in [8]. The application of Glover's method for ANC was proposed in [9] for automotive applications. This technique will be analyzed and simulated in this paper.

When the frequencies of the reference sinusoids are close together, a long filter is required to achieve good resolution between adjacent frequencies [7]. This is an undesired solution for practical applications since a higher-order adaptive filter results in slower convergence, higher excess mean-square error, and higher numerical errors [1]. The relationship between the convergence and the frequency separation is first derived using two complex reference signals with two separated filters; each filter has a complex coefficient [10]. In this paper, we analyze the more practical case of using multiple real-valued sinusoids with a single high-order real-valued adaptive filter. The theoretical analysis shows that the convergence speed increases with an increase in the frequency separation. The analysis also proves that a lower-order filter is sufficient to achieve the same convergence speed for larger frequency separations. These theoretical results are verified by computer simulations.

2. NARROWBAND FEEDFORWARD ANC SYSTEMS

Figure 1 depicts the block diagram for a narrowband feedforward ANC system based on the FXLMS algorithm. Here, $P(z)$ is the primary path, $\hat{S}(z)$ is the estimate of the secondary path $S(z)$. A synchronization signal triggers the multiple-sinewave generator that produces the reference signal $x(n)$, which is filtered by the adaptive filter $W(z)$ to produce the anti-noise $y(n)$ to cancel the primary noise $d(n)$. The secondary signal $y(n)$ is generated as

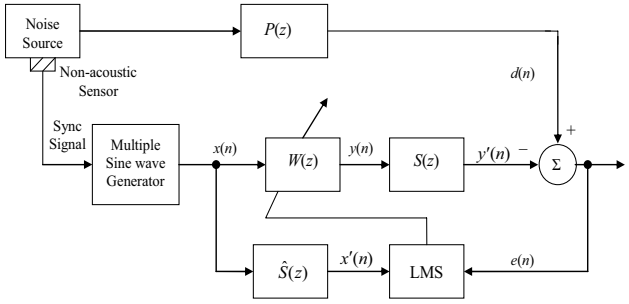

Figure 1 Block diagram of narrowband ANC system.

$$y(n) = \mathbf{w}^T(n)\mathbf{x}(n), \tag{1}$$

where $\mathbf{w}(n) = [w_0(n)\ \ w_1(n) \cdots w_{L-1}(n)]^T$ is the weight vector of $W(z)$, and $\mathbf{x}(n) = [x(n)\ \ x(n-1) \cdots x(n-L+1)]^T$ is the reference signal vector. The filter length L is at least twice the total number of sinusoids because each frequency needs at least two real weights to deal with the in-phase and the quadrature components. The weight vector is updated by the FXLMS algorithm expressed as [1]

$$\mathbf{w}(n+1) = \mathbf{w}(n) + \mu e(n)\mathbf{x}'(n), \tag{2}$$

where μ is the step size, and $\mathbf{x}'(n)$ is the filtered signal vector by $\hat{S}(z)$ as shown in Figure 1.

In the narrowband ANC system proposed in [9], $x(n)$ is the sum of M sinusoids expressed as

$$x(n) = \sum_{i=1}^{M} A_i \cos\{[\omega + (i-1)\Delta\omega]n\}, \tag{3}$$

where $\Delta\omega$ is the frequency separation, A_i is amplitude of the ith

sinusoid at frequency $\omega + i\Delta\omega$ with ω being the fundamental frequency.

For stationary input and sufficiently small μ, the convergence time τ_{mse} is dependent on the eigenvalue spread ρ of the input autocorrelation matrix **R** as [1]

$$\tau_{mse} \le \frac{\lambda_{\max}}{\lambda_{\min}} T_s = \rho T_s \quad \text{(seconds)}, \tag{4}$$

where T_s is the sampling period. In this paper, we will show that the realization of multiple notches requires a higher-order adaptive filter with slow convergence especially when the frequencies of the reference sinusoids are close [7]. The convergence of this ANC system will be analyzed by studying the relationship between the eigenvalue spread ρ and the frequency separation $\Delta\omega$, and the required filter length for a given $\Delta\omega$.

3. ANALYSIS OF DIRECT-FORM ANC SYSTEMS

In this section, we will first derive the exact eigenvalue spread for $M = 2$. Then, we will obtain bounds for the extreme eigenvalues, and the eigenvalue spread for the number of sinusoids $M > 2$. Since our main focus is to study the relationship among the frequency separation, filter length, and eigenvalue spread, we assume the secondary path $S(z)$ is equal to unity for our analysis.

3.1. Convergence Analysis for $M = 2$

The input autocorrelation matrix **R** has dimension LxL, and can be expressed as [1]

$$\mathbf{R} = E\left[\mathbf{x}(n)\mathbf{x}^T(n)\right] = \begin{bmatrix} r_{xx}(0) & r_{xx}(1) & \cdots & r_{xx}(L-1) \\ r_{xx}(1) & r_{xx}(0) & & \vdots \\ \vdots & & \ddots & r_{xx}(1) \\ r_{xx}(L-1) & \cdots & r_{xx}(1) & r_{xx}(0) \end{bmatrix}, \tag{5}$$

where the autocorrelation coefficients $r_{xx}(k)$ are

$$r_{xx}(k) = E[x(n)x(n-k)]. \tag{6}$$

Substituting $x(n)$ defined in (3) into (6), we obtain

$$r_{xx}(k) = \frac{1}{2}\sum_{i=1}^{M} \cos\{[\omega + (i-1)\Delta\omega]k\}. \tag{7}$$

When $M = 2$, the eigenvalue spread can be derived as [11]

$$\rho = \frac{\frac{L}{2} + \sum_{i=1}^{L/2} \cos\left[(2i-1)\Delta\omega/2\right]}{\frac{L}{2} - \sum_{i=1}^{L/2} \cos\left[(2i-1)\Delta\omega/2\right]} \quad \text{for } L \text{ is even.} \tag{8}$$

$$\rho = \frac{\frac{(L+1)}{2} + \sum_{i=1}^{(L-1)/2} \cos(i\Delta\omega)}{\frac{(L-1)}{2} - \sum_{i=1}^{(L-1)/2} \cos(i\Delta\omega)} \quad \text{for } L \text{ is odd.} \tag{9}$$

These theoretical results can be verified and illustrated by observing the variation of eigenvalue spread ρ and filter length L with changing frequency separation $\Delta\omega$. Figure 2 shows the convergence time in equation (4) versus different frequency separations for $L = 4$, i.e., the relation between the theoretical and computed eigenvalue spreads for different frequency separations. The theoretical results are computed using (8) that are identical to the computed results obtained by computing the eigenvalues of (5) using MATLAB. Figure 2 clearly shows the convergence time decreases as the frequency separation increases.

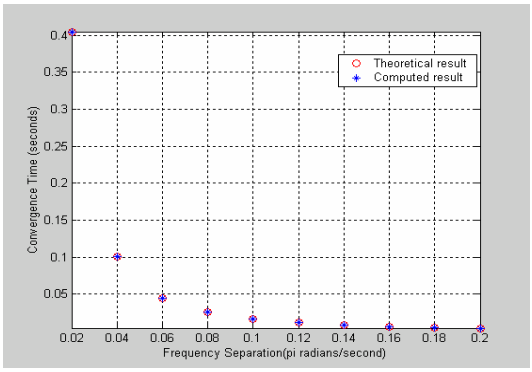

Figure 2 Convergence time vs. different frequency separations for $L = 4$ (even).

Equations (8) and (9) also show that a lower-order filter is able to achieve the same convergence rate for larger frequency separations. Figure 3 shows that as the frequency separation increases, the same convergence rate (indicated by the eigenvalue spread) can be obtained with a much lower filter length.

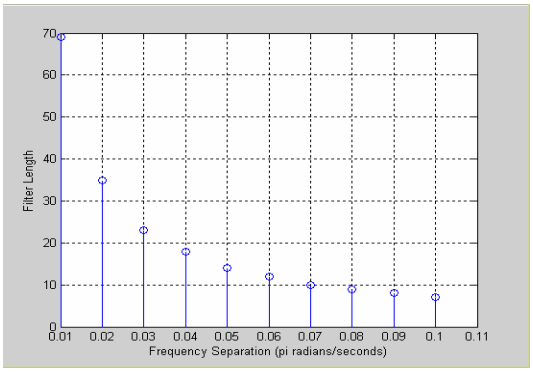

Figure 3 Filter length vs. frequency separation for a fixed eigenvalue spread ρ =10.

3.2. Arbitrary Number of Sinusoids

The matrix **R** can be written as a non-trivial linear combination of M simpler Toeplitz matrices as

$$\mathbf{R} = \frac{1}{2}\sum_{l=1}^{M} \mathbf{R}_l. \tag{10}$$

Each $\mathbf{R}_l$ can be further expressed as

$$\mathbf{R}_l = \mathbf{v}_l\mathbf{v}_l^T + \mathbf{w}_l\mathbf{w}_l^T, \; l = 1, 2, ..., M, \tag{11}$$

where $\mathbf{w}_l$ and $\mathbf{v}_l$ are real-valued Lx1vectors and can expressed as

$$\mathbf{v}_l = [1 \;\; \cos\{\omega + (l-1)\Delta\omega\} \;\; \cos\{2[\omega + (l-1)\Delta\omega]\} \ldots \cos\{(L-1)[\omega + (l-1)\Delta\omega]\}]^T \tag{12}$$

$$\mathbf{w}_l = [0 \;\; \sin\{\omega + (l-1)\Delta\omega\} \;\; \sin\{2[\omega + (l-1)\Delta\omega]\} \ldots \sin\{(L-1)[\omega + (l-1)\Delta\omega]\}]^T. \tag{13}$$

$\mathbf{R}_l$ is a positive semi-definite matrix, thus all its eigenvalues are non-negative. $\mathbf{R}_l$ has rank exactly equal to two and has at most two nonzero eigenvalues. These two nonzero eigenvalues can be computed as [11]

$$\lambda_{1,2} = \frac{1}{2}\left[L \pm \frac{\sin\{L[\omega + (l-1)\Delta\omega]\}}{\sin[\omega + (l-1)\Delta\omega]} \right]. \quad (14)$$

If $\mathbf{R}_l$ is a matrix of rank one, it would have only one nonzero eigenvalue and that is $\lambda = L$.

3.3 Bounds on Extreme Eigenvalues of R

Let $\lambda^+_{\max}$ and $\lambda^+_{\min}$ be the largest and the smallest positive eigenvalues of **R**, respectively. Let $\mathbf{A} \in \Re^{L \times L}$ be a real symmetric matrix. Since **A** is a symmetric matrix, all its eigenvalues are real. Let $\lambda_1, \lambda_2, \lambda_3, \ldots, \lambda_L$ ($\lambda_1 \geq \lambda_2 \geq \lambda_3 \geq \ldots \lambda_L$) be the eigenvalues of **A** and $\mathbf{q}_1, \mathbf{q}_2, \mathbf{q}_3, \ldots, \mathbf{q}_L$ be the corresponding eigenvectors. **A** is a linear combination of mutually perpendicular projection matrices as

$$\mathbf{A} = \mathbf{Q}\Lambda\mathbf{Q}^T = \sum_{i=1}^{L} \lambda_i \mathbf{q}_i \mathbf{q}_i^T \,. \quad (15)$$

Let $\mathbf{x} \in \Re^L$, it can be written as a linear combination of the orthonormal eigenvectors as

$$\mathbf{x} = \sum_{i=1}^{L} \alpha_i \mathbf{q}_i \,, \quad (16)$$

where α_i, i = 1, 2, …, L are all scalars. Thus,

$$\mathbf{x}^T\mathbf{A}\mathbf{x} = \mathbf{x}^T\mathbf{Q}\Lambda\mathbf{Q}^T\mathbf{x} = \left(\mathbf{Q}^T\mathbf{x}\right)^T \Lambda \left(\mathbf{Q}^T\mathbf{x}\right) = \sum_{i=1}^{L} \lambda_i \left(\mathbf{q}_i^T\mathbf{x}\right)^2$$
$$\leq \lambda_1 \sum_{i=1}^{L} \left(\mathbf{q}_i^T\mathbf{x}\right)^2 \,. \quad (17)$$

Therefore, we obtain

$$\lambda_1 = \mathbf{q}_1^T\mathbf{A}\mathbf{q}_1 = \lambda^+_{\max} = \max_{x \neq 0}\left(\frac{\mathbf{x}^T\mathbf{A}\mathbf{x}}{\mathbf{x}^T\mathbf{x}} \right). \quad (18)$$

Similarly, it can be shown that

$$\lambda_L = \mathbf{q}_L^T\mathbf{A}\mathbf{q}_L = \min_{x \neq 0}\left(\frac{\mathbf{x}^T\mathbf{A}\mathbf{x}}{\mathbf{x}^T\mathbf{x}} \right). \quad (19)$$

To find a bound on the largest eigenvalue of the matrix **R**, we use equations (10), (14) and (18) as

$$\lambda^+_{\max} = \max_{\mathbf{x} \neq 0} \frac{\mathbf{x}^T\mathbf{R}\mathbf{x}}{\mathbf{x}^T\mathbf{x}} = \frac{1}{2} \max_{\mathbf{x} \neq 0} \sum_{l=1}^{M} \frac{\mathbf{x}^T\mathbf{R}_l\mathbf{x}}{\mathbf{x}^T\mathbf{x}}$$
$$\leq \frac{1}{2}\sum_{l=1}^{M} \max_{\mathbf{x} \neq 0} \frac{\mathbf{x}^T\mathbf{R}_l\mathbf{x}}{\mathbf{x}^T\mathbf{x}} = \frac{1}{4}\sum_{l=1}^{M}\left[L + \left| \frac{\sin\{L[\omega + (l-1)\Delta\omega]\}}{\sin[\omega + (l-1)\Delta\omega]} \right| \right]. \quad (20)$$

Therefore, we have

$$\lambda^+_{\max} \leq \frac{1}{4}\sum_{l=1}^{M}\left[L + \left| \frac{\sin\{L[\omega + (l-1)\Delta\omega]\}}{\sin[\omega + (l-1)\Delta\omega]} \right| \right] = \mathbf{Z}_1. \quad (21)$$

Let $\mathbf{x}_1$ denote an eigenvector of $\mathbf{R}_{l_1}$ corresponding to its largest eigenvalue, we then have

$$\lambda^+_{\max} = \max_{\mathbf{x} \neq 0} \frac{\mathbf{x}^T\mathbf{R}\mathbf{x}}{\mathbf{x}^T\mathbf{x}} \geq \frac{\mathbf{x}_1^T\mathbf{R}\mathbf{x}_1}{\mathbf{x}_1^T\mathbf{x}_1} \geq \frac{\mathbf{x}_1^T\mathbf{R}_1\mathbf{x}_1}{\mathbf{x}_1^T\mathbf{x}_1}$$
$$\geq \frac{1}{4}\left[L + \left| \frac{\sin\{L[\omega + (l_1-1)\Delta\omega]\}}{\sin[\omega + (l_1-1)\Delta\omega]} \right| \right]. \quad (22)$$

Therefore, we have

$$\lambda^+_{\max} \geq \frac{1}{4}\left[L + \left| \frac{\sin\{L[\omega + (l_1-1)\Delta\omega]\}}{\sin[\omega + (l_1-1)\Delta\omega]} \right| \right] = \mathbf{Z}_2. \quad (23)$$

Equation (19) gives a relation for the minimum eigenvalue of **R**. However, if $L >> 2M$, which is the case when the sinusoids are very close, **R** is a rank deficient matrix. Thus, the minimum eigenvalue would be zero. Hence, we obtain a different bound for the minimum positive eigenvalue. We can use the monotonic theorem in order to obtain a suitable bound for the minimum positive eigenvalue [12]. From (10), we have

$$\mathbf{R} = \frac{1}{2}\mathbf{R}_{l_1} + \frac{1}{2}\sum_{l=1, l \neq l_1}^{M} \mathbf{R}_l = \mathbf{A} + \mathbf{B}\,, \quad (24)$$

where $l = l_1$ such that

$$\max_{1 \leq l \leq M} \left| \frac{\sin\{L[\omega + (l-1)\Delta\omega]\}}{\sin[\omega + (l-1)\Delta\omega]} \right| = \left| \frac{\sin\{L[\omega + (l_1-1)\Delta\omega]\}}{\sin[\omega + (l_1-1)\Delta\omega]} \right|. \quad (25)$$

Let p be the rank of the matrix **R**. There are p nonzero eigenvalues and ($L - p$) zero eigenvalues such that $\lambda_1 \geq \lambda_2 \geq \ldots \geq \lambda_p > 0$ and $\lambda_{p+1} = \ldots = \lambda_L = 0$.

Let the eigenvalues of **B** in equation (24) be $\beta_1 \geq \beta_2 \geq \ldots \geq \beta_L$. The matrix **A** in equation (24) has only two nonzero eigenvalues α_1 and α_2 expressed as

$$\frac{1}{2}\left[L + \left| \frac{\sin\{L[\omega + (l-1)\Delta\omega]\}}{\sin[\omega + (l-1)\Delta\omega]} \right| \right] \geq \frac{1}{2}\left[L - \left| \frac{\sin\{L[\omega + (l-1)\Delta\omega]\}}{\sin[\omega + (l-1)\Delta\omega]} \right| \right] > 0. \quad (26)$$

From the monotonic theorem, we have

$$\lambda_p = \lambda^+_{\min} \leq \alpha_2 + \beta_{p-1}$$
$$= \frac{1}{4}\left[L - \left| \frac{\sin\{L[\omega + (l_1-1)\Delta\omega]\}}{\sin[\omega + (l_1-1)\Delta\omega]} \right| \right] + \beta_{p-1}. \quad (27)$$

Each of the matrices $\mathbf{R}_l$ has rank two. Thus, the rank of the matrix **B** in the equation (24) has a rank of at most 2(M–1). From equation (27), we have

$$\lambda^+_{\min} \leq \frac{1}{4}\left[L - \left| \frac{\sin\{L[\omega + (l_1-1)\Delta\omega]\}}{\sin[\omega + (l_1-1)\Delta\omega]} \right| \right] = \mathbf{Z}_3\,. \quad (28)$$

Equations (21), (23) and (28) give the bounds on the largest and the smallest positive eigenvalues of **R**. It shows the bounds $\mathbf{Z}_1$, $\mathbf{Z}_2$, and $\mathbf{Z}_3$ depend on the frequency separation $\Delta\omega$. $\mathbf{Z}_1$ and $\mathbf{Z}_2$ decrease with an increase in the frequency separation while $\mathbf{Z}_3$ increases. The oscillatory behavior is explained by the dampening sinusoidal component in each of the bounds given in equations (23) and (28). The bound decreases with an increase in the frequency separation. Therefore, we proved that the convergence speed is dependent on the frequency separation for an arbitrary value of M.

3.4 Computer Simulations

Computer simulations are performed to observe the effect of frequency separation on eigenvalue spread and to validate the theoretical analysis for arbitrary number of sinusoids. The simulation results for M equals 4, 8, and 16 with the filter length $L = 2M$ are illustrated in Figure 4. This figure shows eigenvalue spread decreases with an increase in frequency separation.

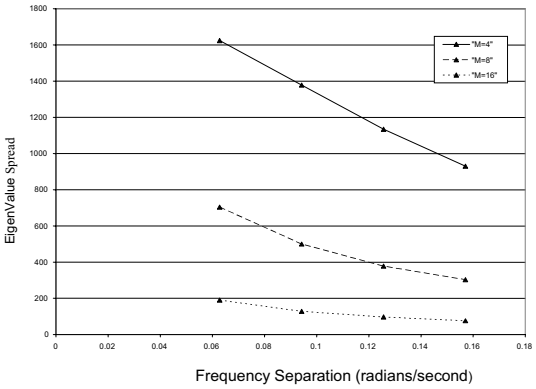

Figure 4 Eigenvalue spread vs. frequency separation.

Figure 5 shows that filter length affects the eigenvalue spread and thus the rate of convergence. For a given number of sinusoids ($M = 4$), the eigenvalue spread is computed for the filter length of 8, 12 and 16. For a given frequency separation Δf, an increase in filter length decreases the eigenvalue spread and increases the rate of convergence. This also implies that the filter length needs to be increased as the frequency separation decreases in order to achieve the same rate of convergence.

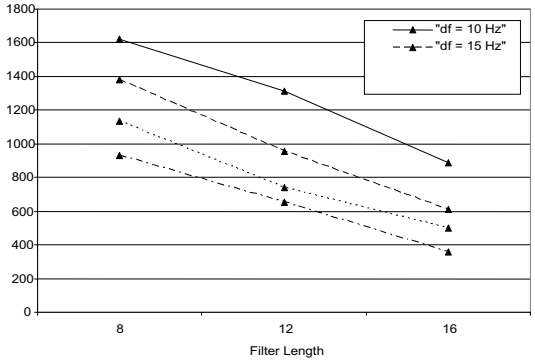

Figure 5 Effect of filter length on eigenvalue spread with different frequency separations.

For a given frequency separation and the number of sinusoids M, the learning curve is obtained. The plots for different frequency separations are shown in the Figure 6. The simulations are performed for four different frequency separations: 10 Hz, 15 Hz, 20 Hz, and 25 Hz with the sampling rate of 2 kHz. The total number of sinusoids is $M = 8$ and the filter length is $L = 128$. This simulation clearly shows that the rate of convergence increases with an increase in the frequency separation for $M = 8$, and it can also be extended for arbitrary values of M

4. CONCLUSIONS

This paper analyzed the convergence of narrowband ANC with multiple sinusoidal frequency components. The relationship involving frequency separation between adjacent harmonics, eigenvalue spread, and filter length is derived. This analysis showed faster convergence can be achieved for larger frequency separation in the reference signal. This paper also proved that the filter length required for achieving the same convergence speed decreases with an increase in the frequency separation.

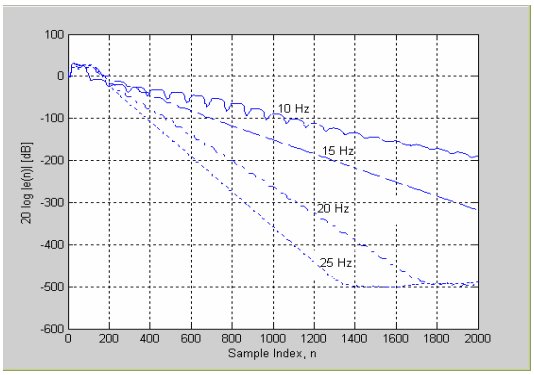

Figure 6 Learning curves for frequency separation of 10, 15, 20 and 25Hz

References:

[1] S. M. Kuo and D. R. Morgan, *Active noise control systems – Algorithms and DSP implementations*, New York, NY: John Wiley & Sons, Inc., 1996.

[2] S. M. Kuo and D. R. Morgan, Active noise control: A tutorial review, *Proc. of the IEEE,* vol. 8, no. 6, pp. 943-973, June 1999.

[3] G. W. B. Chaplin, "The cancellation of repetitive noise and vibration," in *Proc. Inter-Noise*, pp. 699-702, Dec. 1980.

[4] S. J. Elliott and P. Darlington, "Adaptive cancellation of periodic, synchronously sampled interference," *IEEE Trans. on Acoust., Speech Signal Processing,* vol. ASSP-33, no. 3, pp. 715-717, June 1985.

[5] D. R. Morgan, "An analysis of multiple correlation cancellation loops with a filter in the auxiliary path," *IEEE Trans. on Acoust., Speech Signal Processing*, vol. ASSP-28, no. 4, pp. 454-467, Aug. 1980.

[6] B. Widrow, et. al., "Adaptive noise canceling: Principles and applications", *Proc. of IEEE*, vol. 63, pp. 1692 – 1716, Dec. 1975.

[7] J. R. Glover, "Adaptive noise canceling applied to sinusoidal interferences," *IEEE Trans. on Acoustics, Speech, and Signal Processing*, vol. ASSP-25, no. 6, pp. 484-491, Dec. 1977.

[8] S. J. Elliott and P. A. Nelson, "The application of adaptive filtering to the active control of sound and vibration," ISVR Technical Report No. 136, Sept. 1985.

[9] D. P. Pfaff, N. S. Kapsokavathis, and N. A. Parks, "Method for actively attenuating engine generated noise," U. S. Patent No. 5,146,505, Sept. 8, 1992.

[10] S. Johansson, S. Nordebo, and I. Claesson, "Convergence analysis of a twin-reference complex least-mean-square algorithm," *IEEE Trans. Speech and Audio Processing*, vol. 10, no. 4, pp. 213-221, May 2002.

[11] A. B. Puvvala, *Effects of frequency separation on rate of convergence in multiple-frequency periodic noise control systems*, MS thesis, Northern Illinois University, December 2004.

[12] C. R. Rao and M. B. Rao, *Matrix algebra and its applications to statistics and econometrics,* Singapore: World Scientific Publishing Co 1998.